

# Geophysical Investigation Of Groundwater Potential And Susceptibility In North Bank, Makurdi, North Central, Nigeria

T. Igbawua<sup>1</sup>, J. T. Jonah<sup>1</sup>, T. Emberga<sup>1</sup>, D.T. Ayaakaa<sup>2</sup>

<sup>1</sup>(Department Of Physics, College Of Physical Sciences, Joseph Sarwuan Tarka University, Makurdi, Nigeria)

<sup>2</sup>(Department Of Physics, Faculty Of Science/ Benue State University Makurdi, Nigeria)

---

## ABSTRACT:

In order to address the growing demand for clean, fresh water for industrial or domestic use, a geophysical survey utilizing the Vertical Electrical Sounding (VES) and laboratory technique was conducted to assess groundwater potential and vulnerability of Makurdi North Central Nigeria's North Bank Areas. Fifteen (15) VES in all were conducted using four to five geoelectric layers, with five layer types appearing most frequently in the fourth layer, which is the aquifer zone. The aquifer's thickness and resistivity range from 7.70 to 155.60 m and 20.80 to 209.60  $\Omega\cdot m$ , respectively, with an average value of 44.47 m and 93.34  $\Omega\cdot m$ . With an average value of 0.65  $\Omega\cdot m^{-1}$ , 4618.51  $\Omega m^2$ , 7.90m/day, 332.33m<sup>2</sup>/day, 33.97%, and 11.50m/day, respectively, the calculated longitudinal conductance, transverse resistance, hydraulic conductance, transmissivity, porosity, and coefficient of permeability range from 0.22 to 1.76 $\Omega\cdot m^{-1}$ , 160.16 to 13739.48  $\Omega m^2$ , 2.64 to 22.78m/day, 114.21 to 92002m<sup>2</sup>/day, 29.87 to 39.57%, and 1.40 to 30.25m/day. The study area comprises sandy loam soil with approximately 80% of moderately protected aquifers, making the aquifer susceptible to contamination. Using laboratory methods, ten water samples from hand-dug wells and existing boreholes in the research region were examined. With average values of 29.810C, 6.98, 220.83mg/l, 366.40  $\mu S/cm$ , 12.10NTU, and 127.30mg/l, respectively, the temperature, pH, TDS, electrical conductivity, turbidity, and total hardness values ranged from 26.00 to 32.70<sup>o</sup>C, 6.51 to 7.25, 66.30 to 300.00mg/l, 132.00 to 574.00  $\mu S/cm$ , 0.35 to 35.60NTU, and 30.00 to 165.00mg/l. The Calcium, Magnesium, Iron, Copper, Manganese ion values range from 14.00 to 50.00 mg/l, 8.00 to 60.00 mg/l, 0.01 to 0.11 mg/l, 0.03 to 0.15 mg/l, 0.10 to 0.45 mg/l, with an average value of 38.70 mg/l, 31.70 mg/l, 0.04 mg/l, 0.08 mg/l and 0.26 mg/l respectively. There were almost 20% of the cations that had findings above the WHO/NAFDAC 2015 guidelines. Average values for the ions of chlorine, sulfur, nitrate, and nitrite vary from 110.00 to 400.00 mg/l, 8.00 to 95.00 mg/l, 12.00 to 40.00 mg/l, and 0.02 to 0.50 mg/l, respectively. NAFDAC/WHO 2015, a criterion that is reduced to contamination and vulnerability, is exceeded by about 75% of the anion results. In conclusion, a good and high-quality water supply should be obtained from hand-dug wells and boreholes 150 meters above sea level within the research region.

**Key Word:** Geoelectric lateral, resistivity, thickness and depth of subsurface, aquifer parameters, aquifer vulnerability, metallic substances

---

Date of Submission: 16-12-2023

Date of Acceptance: 26-12-2023

---

## I. Introduction

Groundwater is a key natural resource that is held in subterranean geological formations in the critical zone of the earth's crust<sup>1</sup>. Groundwater is a critical resource for current and future generations, but it is not being used in many regions of the world in a sustainable manner<sup>2</sup>. Exploration of groundwater has been the most reliable means to meet the ever-increasing need for fresh and high-quality water for household, agricultural, and industrial applications. This is due to its greater availability and quality in comparison to many other sources. The development of this vital resource in Nigeria has not produced an amazing outcome commensurate with the financial resources invested<sup>3</sup>. As a result, a large proportion of the inhabitants in this nation are unable to get safe drinking water. According to Perdomo et al.<sup>4</sup>, insufficient funds have also impeded the distribution of water and the availability of critical information to assist in appraising this resource in poor nations.

Exploration of this vital material necessitates the use of several geographical and hydrogeological techniques such as electrical resistivity, seismic, magnetic, electromagnetic, ground probing radar, pumping tests, and down-hole logging<sup>5</sup>. The electrical resistivity approach has been a very important tool in investigating the earth for groundwater<sup>6</sup>. Electrical resistivity has been extensively used to study or probe the earth's underlying layers. This is due to its ability to discern between sandy and clayey formations, porous and impermeable rock, and fresh and saline water aquifers. It is utilized to collect information about the underlying

layers and the location of groundwater<sup>7</sup>. The difference in electrical resistivity of several lithological sequences in the subsurface is utilized to identify the subsurface layers and estimate the area's groundwater potential<sup>8</sup>. Groundwater is the water that occurs under the water table in the pore spaces and cracks of rocks and sediment. It is formed by rain and melting snow that percolates downward from the surface; it gathers in the open pores gaps between soil particles or in cracks and fissures in bedrock, eventually making its way back to the surface streams, lakes, or seas<sup>9</sup>.

Since the soil and rocks through which groundwater runs screen off the majority of the germs, groundwater is less vulnerable to bacterial contamination than surface water. However, the absence of bacterial contamination does not guarantee that the water is safe to drink<sup>10, 11</sup>. Many invisible dissolved mineral and organic elements exist in varying amounts in groundwater. Most of them are safe or even useful; however, some are dangerous, and a few may be severely poisonous, and may be discovered using laboratory procedures<sup>12</sup>. Because groundwater is the most favoured source of water for home, agricultural, and industrial applications, we must provide effective exploration, appraisal, monitoring, and management of this vital resource to assure its quality and availability.

Surface water quality is commonly found to be significantly deteriorated as a result of exposure to physical, biological, or chemical compounds<sup>13</sup>. Even with the availability of the Benue River, the insufficient supply of drinkable water on Makurdi's North bank is getting worse by the day. This is due to the lack of public water supply, as well as the growing problem of individuals not obtaining water from sanitary sources. People's primary supply of water has been surface water, which is prone to contamination. As a consequence of the current challenges connected with these sources of water to meet household demands, it has become necessary to conduct a geophysical study to allow inhabitants of Makurdi's North Bank to access good-quality water to suit their domestic needs.

Pit latrines and dumpsites are being built in Makurdi's North Bank without regard for the area's hydrogeological conditions, putting groundwater's future in danger. Furthermore, the use of chemical products in farms, such as pesticides and herbicides, as well as the dumping of significant quantities of waste materials, raises the potential danger of widely dispersed groundwater contamination in the study region. These toxins endanger the health of the individuals in the region.

Several researches have been carried out on ground water potential in Nigeria. A study of groundwater potential in the neighbourhood of the Gidan Kwano campus of the Federal University of Technology, Minna by Amadi *et al.*<sup>14</sup> was carried out using vertical Electrical resistivity sounding. Adeniji *et al.*<sup>15</sup> investigated the groundwater potentials of the Bwari basement area using solely geoelectric surveys. Akande *et al.*<sup>16</sup> evaluated the groundwater potential of the Chanchaga area of Minna, North central Nigeria. A total of 10 VES-sounding surveys were carried out in Anyigba and its environs, Kogi state, to delineate the aquifer potential by Onimisi *et al.*<sup>17</sup>.

In the context of Makurdi, Benue State, various studies have been conducted to explore the groundwater potential in both the north and south banks of the city. Obiora<sup>18</sup> delved into an investigation of groundwater flow potential in Makurdi, utilizing Vertical Electrical Sounding (VES) with the Schlumberger electrode design. The outcomes of this study revealed detailed thickness and transmissivity distribution maps, facilitating the identification of locations abundant in the aquiferous zone. Building upon this research, Obriake *et al.*<sup>19</sup> extended their study to the North Bank and its vicinity in Makurdi, Benue State. Employing 21 Vertical Electrical Soundings (VES) with the Schlumberger electrode array and ABEM Terrameter, they aimed to determine the depth of the aquifer, aquifer thickness, groundwater potential, and aquifer vulnerability in the region. On the southern bank of the Makurdi River, Ayaakaa *et al.*<sup>20</sup> conducted a comprehensive assessment of the geoelectrical parameters to evaluate the groundwater potentials of specific areas within the Makurdi Metropolis. Their approach involved utilizing the Dar Zarrouk Parameters to gain insights into the hydrogeological conditions of the region. In the southern bank, Akuh<sup>21</sup> and Musa<sup>22</sup> contributed to the understanding of the geology and hydrogeology of Part of Makurdi Sheet 251 SW, North Central Nigeria. These studies collectively provide a holistic perspective on the groundwater dynamics in Makurdi, contributing essential information for effective water resource management in the region.

Existing literature indicates a noticeable gap in comprehensive geophysical research concerning groundwater potential and vulnerability in the North Bank area of Makurdi River. While Obiora<sup>18</sup> and Obriake *et al.*<sup>19</sup> conducted extension studies on groundwater flow potential, their investigations did not encompass in situ measurements from hand-dug wells and surface waters to determine the physicochemical parameters. Consequently, this research aims to address this gap by undertaking a geophysical survey of groundwater potential in the North Bank area of Makurdi, Benue State, Nigeria, utilizing electrical resistivity. Additionally, the study aims to measure the physiochemical characteristics of groundwater in the same area, providing a more comprehensive understanding of the hydrogeological conditions in the region. This research is pivotal for enhancing our knowledge of the local groundwater system and will contribute valuable insights for sustainable water resource management in the study area.

## II. Material And Methods

### *Location and geology of the study area*

The study area, North Bank in the Makurdi Local Government Area of Benue State, North Central Nigeria (Figure 2), is positioned between latitudes 7°46'14"N and longitude 8°33'38"E, encompassing a total area of approximately 670 km<sup>2</sup>. The locations of the Vertical Electrical Sounding (VES) points are detailed in Table 1. Makurdi is situated within the Guinea savannah vegetation zone, featuring a few patches of forests. The annual rainfall varies between 1,500 to 2,000 mm, reaching its peak in July. Temperatures in March and April range from about 38 to 48°C, while in December and January, the temperature is around 27°C. Makurdi is part of the Makurdi Formation, overlaying the Albian Shale. This formation consists of thick, currently bedded coarse-grained deposits, with the Makurdi sandstone measuring approximately 900 m in thickness<sup>23</sup>.

### *Satellite Data*

The satellite data utilized in this study include (1) the Digital Elevation Model (DEM) and (2) the United States Department of Agriculture (USDA) soil profile maps. The DEM was acquired from resampled SRTM data, with a spatial resolution of approximately 250 meters, provided by the Consultative Group on International Agricultural Research (CGIAR) Consortium for Spatial. The USDA soil data was sourced from Zenodo records<sup>24</sup>. The USDA soil texture information of the study area is given in figure 3.

**Table 1** Location of VES points

VES points	Location	Latitude	Longitude
1	UAM College of Science Block South Core N/B	7.7649	8.6239
2	UAM Farm House North Bank	7.7622	8.6239
3	UAM Research Farm North Bank	7.7580	8.6238
4	UAM Fish Pond South Core	7.7528	8.6206
5	UAM College of Engineering Complex Middle Core	7.7918	8.6206
6	UAM College of Mgt Sciences	7.7919	8.6183
7	UAM Soil Science Met. St. North Core	7.7457	8.6097
8	UAM Postgraduate Sch. North Core	7.7958	8.6131
9	Our Lady of Fatima Pri. Sch., Federal Housing Estate	7.7554	8.5711
10	Federal Low Cost Housing Estate	7.7798	8.5428
11	LGEA Pri. School North Bank	7.7581	8.5428
12	Okwute Well North Bank	7.7516	8.5425
13	Patrick Ogbuh Street Hudco Qtrs North Bank	7.7480	8.5606
14	Dave Memorial Sec. Sch. North Bank	7.7540	8.5606
15	Nigerian Police Force Station "C" Division N/B	8.0074	8.5664

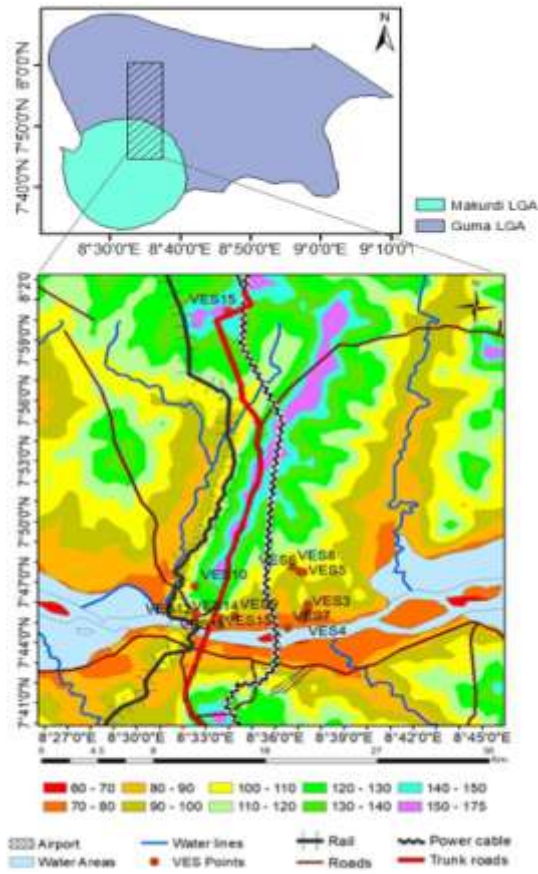


Figure 2 Topographic map of the study area showing VES points and digital elevation model (DEM) in meters

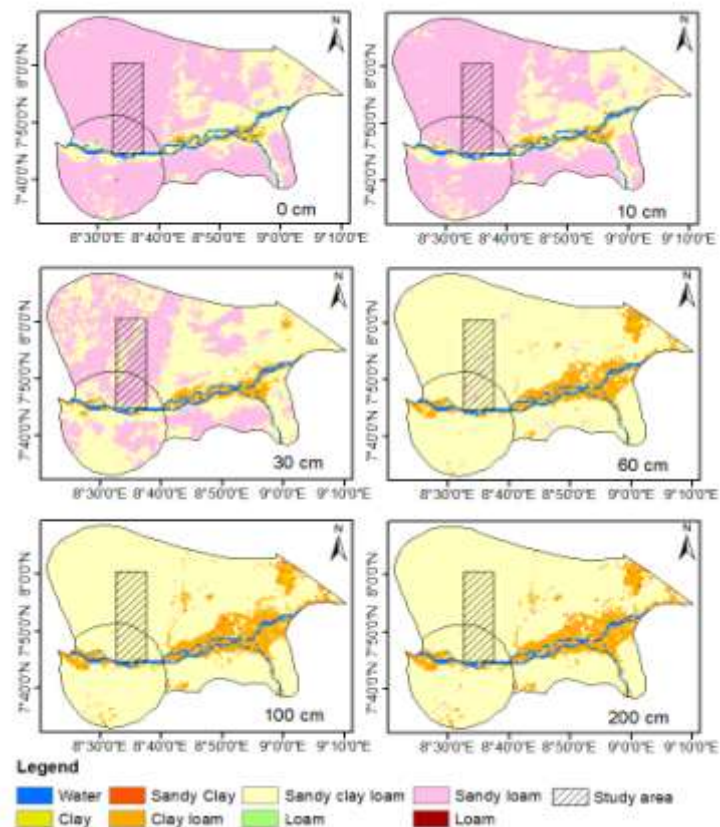


Figure 3 United States Department for Agriculture (USDA) soil profile of study area from 0 to 200 cm

**Methods**

In this study, electrical resistivity tests were taken along relatively straight streets, paths, and areas left fallow for bushes. It made use of the Schlumberger electrode configuration (Figure 4). A total of fifteen VES were performed in the research location, with a half current electrode separation of 300 m and a half potential electrode spacing of 10 m. The ground was connected to the ultra MiniRes40 resistivity meter using a set of potential electrodes and insulated wires. Five steel electrodes were used to make enough electrical contact with the Earth and were pushed into the ground to roughly a third of the electrode's length.

Field permeability pits were dug in a few important locations around the research area. Each pit was around 10 by 10 by 10 cm. The hole was filled with 250cm<sup>3</sup> of water. A timer was used to record how long it took for the water to infiltrate the underlying soil entirely. This experiment was repeated five times in a particular pit. The Darcy formula (10) was used to calculate the soil's K<sub>p</sub> coefficient of permeability in the research region. The stenzel table can be used to identify the soil type. Electrical resistance is inherent in all materials. The method includes injecting purposefully produced electrical currents into the ground and then measuring the potential differences that result at the surface.

Field permeability pits were dug in a few important locations around the research area. Each pit was around 10 by 10 by 10 cm. The hole was filled with 250 cm<sup>3</sup> of water. A timer was used to record how long it took for the water to infiltrate the underlying soil entirely. This experiment was repeated five times in a particular pit. The Darcy formula (10) was used to calculate the soil's K<sub>p</sub> coefficient of permeability in the research region. The stenzel table can be used to identify the soil type. Electrical resistance is inherent in all materials. The method includes injecting purposefully produced electrical currents into the ground and then measuring the potential differences that result at the surface.

The method includes injecting purposefully produced electrical currents into the ground and then measuring the potential differences that result at the surface. Electrical resistivity measurements were taken along relatively straight roadways, footpaths, and wide fields of bushes. It made use of the Schlumberger electrode configuration. A total of fifteen VES were performed in the research location, with a half current electrode separation of 300 m and a half potential electrode spacing of 10 m. Two potential electrodes and insulated cables were used to make an electrical connection between the resistivity meter and the ground. Five steel electrodes were used. Five steel electrodes were used to make enough electrical contact with the Earth and were pushed into the ground to roughly a third of the electrode's length.

The Schlumberger array comprises two electrodes with identical potential and current midway. The potential electrodes are momentarily fixed while the current electrodes are extended symmetrically about the middle. Most geo-electric surveys employ the Schlumberger array because it has a higher resolution and needs less effort than other designs. The MiniRes 40 resistivity meter was used with maximum current electrode spacing  $\left(\frac{AB}{2}\right)$  of 300.0 m,  $\left(\frac{CD}{2}\right)$  of 10.0 m. The resistances of the subsurface were measured and recorded against the appropriate potential and current electrode separation. At the detection electrode "C" the potential due to source A is  $+\rho_a I / (2\pi r_{AC})$  and that due to sink B is  $-\rho_a I / (2\pi r_{CB})$ , the combined potential at C is given as

$$V_c = \frac{\rho_a I}{2\pi} \left( \frac{1}{r_{AC}} - \frac{1}{r_{CB}} \right) \quad (1)$$

The combined potential at D is given as

$$V_D = \frac{\rho_a I}{2\pi} \left( \frac{1}{r_{AD}} - \frac{1}{r_{DB}} \right) \quad (2)$$

Thus the potential difference measured between C and D is

$$V_{CD} = \frac{\rho_a I}{2\pi} \left\{ \left( \frac{1}{r_{AC}} - \frac{1}{r_{CB}} \right) - \left( \frac{1}{r_{AD}} - \frac{1}{r_{DB}} \right) \right\} \quad (3)$$

The ground apparent resistivity ( $\rho_a$ ) can be evaluated as

$$\rho_a = 2\pi \frac{\Delta V}{I} \left\{ \frac{1}{\left( \frac{1}{r_{AC}} - \frac{1}{r_{AD}} \right) - \left( \frac{1}{r_{CB}} - \frac{1}{r_{DB}} \right)} \right\} = K \frac{\Delta V}{I} \quad (4)$$

$$\text{This implies that } K = 2\pi \frac{\Delta V}{I} \left\{ \frac{1}{\left( \frac{1}{r_{AC}} - \frac{1}{r_{AD}} \right) - \left( \frac{1}{r_{CB}} - \frac{1}{r_{DB}} \right)} \right\} = \pi \left\{ \frac{\left(\frac{AB}{2}\right)^2 - \left(\frac{CD}{2}\right)^2}{CD} \right\} \quad (5)$$

where,  $\Delta V = V_{CD}$  and K is geometric factor and is dependent upon the spatial arrangement of electrodes for specific arrays.

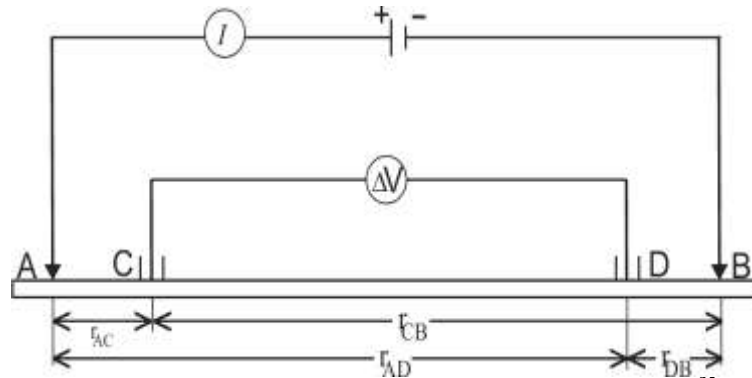


**Figure 4:** The general electrode configuration arrangements<sup>25</sup>

The electrical resistivity curve types matching approaches using two, three, four, and so on layer master curves enabled the earliest estimates of VES data<sup>26</sup>. Estimates of layer resistivities, thickness, and depth were derived to enable computer-assisted interpretation. The use of the master ascending and descending and master two layer auxiliary electrical resistivity curves in the interpretation made it simpler to get a reasonable fit between the observed field curves and the theoretical curves during total and partial matching. The computer modeling program (WINRESIST) was used to generate data for the estimated model, and the data sets received from the manual interpretation stage were entered in as inputs. Table 8 shows how the aquifer thickness and depth were utilized to calculate the geohydraulic parameters. According to Heigold et al.<sup>27</sup>, hydraulic conductivity (H) may be calculated as follows:

$$H = 386.40 \rho_a^{-0.93283} \quad (6)$$

Where, H is the hydraulic conductivity and  $\rho_a$  is the apparent resistivity

The Longitudinal conductance was calculated using<sup>28</sup>:

$$S = \frac{h}{\rho_a} \quad (7)$$

Where, S is longitudinal conductance, h is layer thickness and  $\rho_a$  is layer resistivity.

The total transverse resistances were calculated using<sup>29</sup>:

$$T = \rho_a h \quad (8)$$

Where, T is total transverse resistance,  $\rho_a$  is the apparent resistivity and h is layer thickness.

The transmissivity values were calculated using<sup>30</sup>:

$$T_r = H h \quad (9)$$

Where,  $T_r$  is transmissivity, H is hydraulic conductivity and h is hydraulic conductivity.

The coefficients of permeability were obtained using<sup>31</sup>:

$$K_p = \frac{Q}{AI} \quad (10)$$

Where  $K_p$  is the permeability coefficient, Q is the rate of water discharge through the soil/lithology, A is the cross sectional area of the field permeameter, and I is the hydraulic gradient.

For the evaluation of groundwater vulnerability in the research region, 10 water samples were obtained at random from existing bore, hand dug wells/holes. Temperature, electrical conductivity, total dissolved solids (TDS), turbidity, and PH were among the physical and chemical properties of the water samples collected. Wagtech conductivity/TDS meter (592599) was used to test the temperature, electrical conductivity, and total dissolved solids of the water samples. The turbidity of the water samples was measured with a Wagtech turbidity meter (625235), and the PH was measured with a Wagtech PH meter (618693). Cations, anions, and total hardness were determined in water samples using the photometric technique and reagents.

### III. Result

According to Figure 3, the USDA soil texture values for the 0 to 30 cm depth indicate a predominance of sandy loam soils. However, as we delve deeper, from 60 cm to 200 cm, the prevalent soil type shifts to sandy clay loam.

The field curves derived from the geo-electric data illustrate the correlation between apparent resistivity and half current electrode spacing, as depicted in Figures 5-8. From these figures, values for resistivity, thickness, and depth, along with the identification of curve types, were determined and summarized in Table 2. Aquifer thickness and depth values, extracted from the field curves, were utilized in computing the petrophysical properties associated with groundwater potential, as detailed in Table 3. Concurrently, Table 4 provides the outcomes of the physiochemical characteristics of groundwater within the study area. A comparative analysis with NAFDAC/WHO<sup>32,33</sup> standards is presented in Table 5. To visually represent the spatial variations of aquifer thickness, resistivity values, longitudinal conductance, transverse resistance,

hydraulic conductivity, transmissivity, porosity, and coefficient of permeability, contour maps were generated using the Surfer 13 software package, as illustrated in Figures 9 and 10.

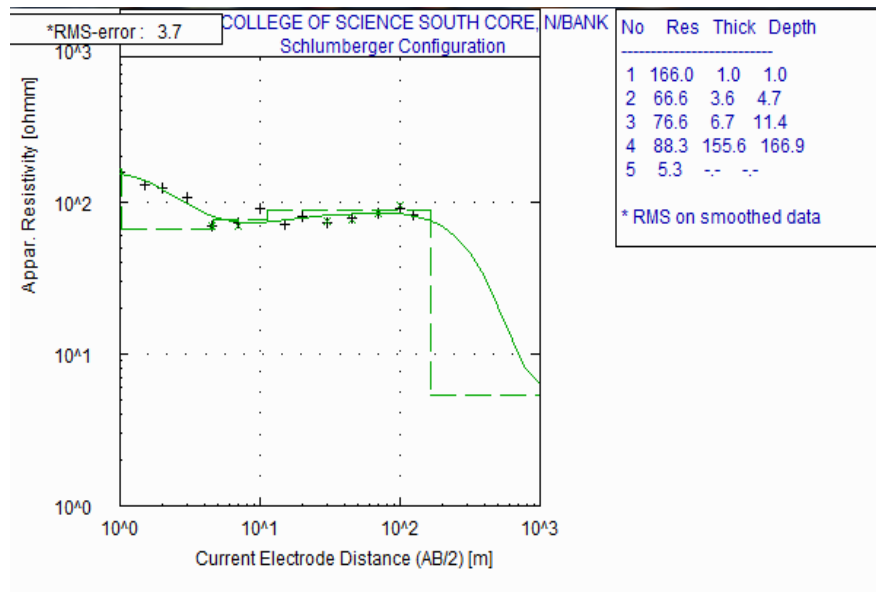


Figure 5: Geo-electric Curve model for VES 1

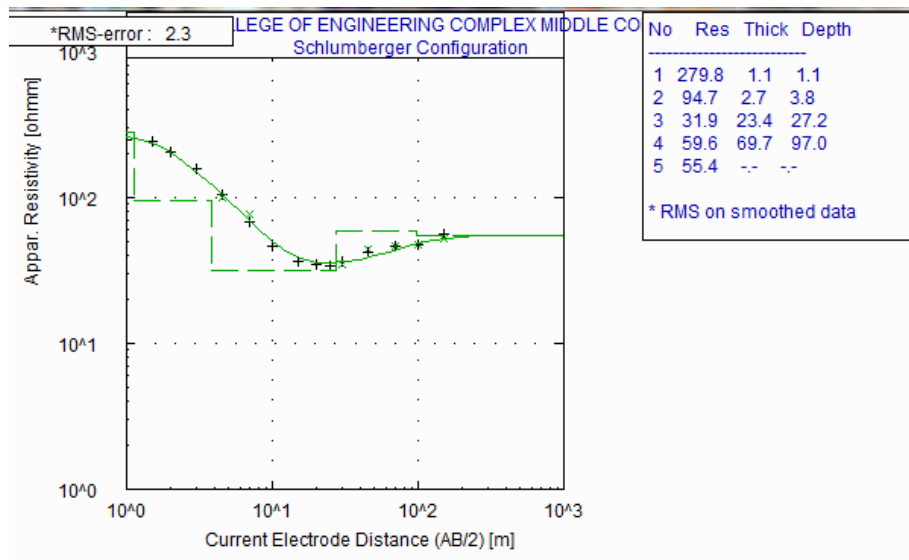


Figure 6: Geo-electric Curve model for VES 5

The findings unveiled a highly heterogeneous subsurface, characterized by the presence of four to five distinct geoelectric layers (refer to Table 2). The results encompass layer resistivities, thicknesses, depths, and the associated curve types, all acquired within the maximum electrode separation at each Vertical Electrical Sounding (VES) point. It's noteworthy that the fifth layer remains undefined in the majority of VES points, except for VES 13 where the fourth layer is indeterminate. The observed variation in resistivity values across the study area suggests that the lithology of the top layer is predominantly composed of materials with low to medium resistivity.

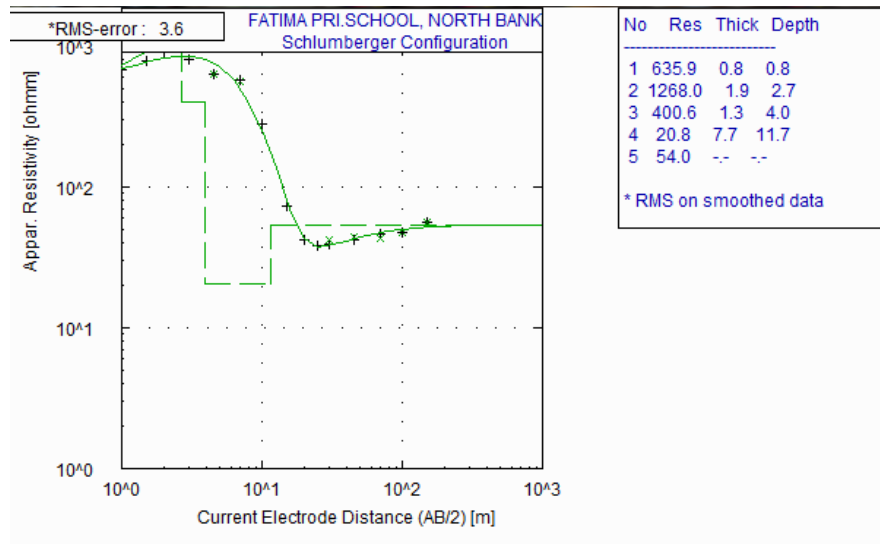


Figure 7: Geo-electric Curve model for VES 9

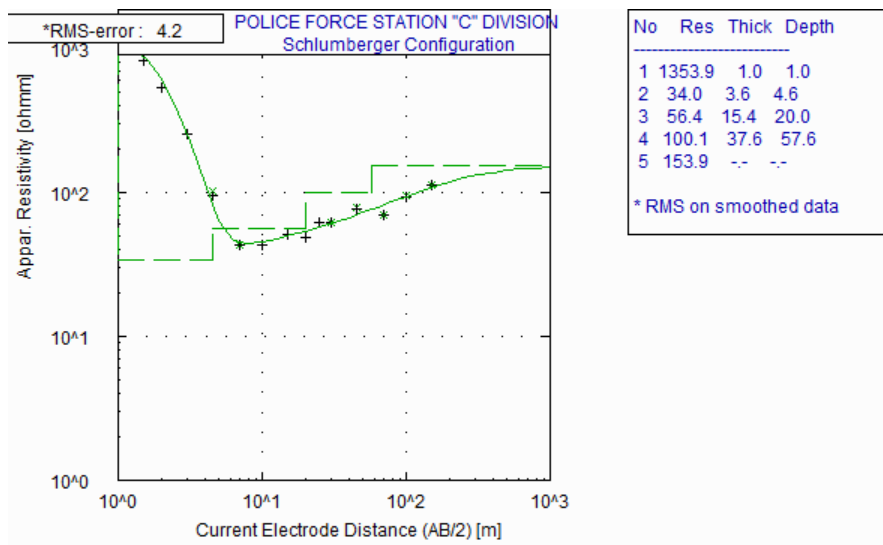


Figure 8: Geo-electric Curve model for VES 15

The lateritic topsoil, characterized by resistivity ranging from 34.0 to 1458.1  $\Omega$ m, indicates the presence of sand with a progressive increase at certain Vertical Electrical Sounding (VES) points. The thickness and depth of the top layer vary from 0.3 to 2.6 m. This top layer's nature enhances rainwater infiltration into the subsurface aquifer units. The second layer is dominated by low to medium resistivity materials, with resistivity values ranging from 12.6  $\Omega$ m at VES 4 to 7802.2  $\Omega$ m at VES 14. The thickness and depth of this layer vary from 1.2 to 5.3 m and 1.4 to 6.8 m, respectively. Underlying the second layer is a relatively thick layer (layer 3) with resistivity values ranging from 12.4  $\Omega$ m at VES 6 to 400.6  $\Omega$ m at VES 14, being relatively more conductive than the topmost layer. The low resistivity observed in the underlying layers may be attributed to the presence of materials such as sandy clay/shale<sup>34</sup>. The thickness and depth of layer 3 vary between 1.3 m at VES 9 to 48.2 m at VES 13, respectively. The fourth layer's resistivity ranges from 20.8  $\Omega$ m at VES 9 to 209.6  $\Omega$ m at VES 12, with thickness and depth varying from 7.7 to 155.6 m and 11.7 to 166.9 m, respectively. This layer is identified as the aquifer layer with relatively low resistivity values and a much thicker layer than the overlain layers, except at VES 13, where the third layer is delineated as the aquifer layer. The fifth layer has resistivity values ranging from 5.3 to 372.6  $\Omega$ m, with thickness and depth undefined in all the VES points. The four-layer geo-electric section is characterized by KH curve type (VES 13), while the five-layer geo-electric sections are characterized by KAQ, QHQ, QHH, KAH, QHQ, QHQ, KAH, KAQ, AKH, HAQ, KAH, KHH, KQH, and HAH curve types for (VES 1, 2, 3, 4, 5, 6, 7, 8, 9, 10, 11, 12, 14, and 15), respectively. These curve types were identified using the standard curve types.



**Table 2:** Summary of the results obtained from interpreted VES data

VES	Layer resistivity ( $\Omega m$ )					Thickness (m)					Depth (m)					Curve type
	$\rho_1$	$\rho_2$	$\rho_3$	$\rho_4$	$\rho_5$	$h_1$	$h_2$	$h_3$	$h_4$	$h_5$	$d_1$	$d_2$	$d_3$	$d_4$	$d_5$	
1	166.0	66.6	76.6	88.3	5.3	1.0	3.6	6.7	155.6	-	1.0	4.7	11.4	166.9	-	KAQ
2	253.2	71.8	68.6	145.7	68.6	1.4	5.3	16.7	36.3	-	1.4	6.8	23.4	59.7	-	QHQ
3	112.3	61.9	49.7	84.8	89.0	1.3	1.9	8.1	18.6	-	1.3	3.2	11.3	29.9	-	QH H
4	1010.0	12.6	14.7	27.6	372.6	0.3	2.8	22.3	16.5	-	0.3	3.1	25.4	42.0	-	KAH
5	279.8	94.7	31.9	59.6	55.4	1.1	3.8	27.2	97.0	-	1.1	3.8	27.2	97.0	-	QH Q
6	34.0	14.0	12.4	37.6	23.2	1.2	3.2	11.0	63.3	-	1.2	4.4	15.4	78.6	-	QH Q
7	60.6	15.0	58.0	67.6	85.4	0.5	2.6	22.8	39.0	-	0.5	3.0	25.8	64.8	-	KAH
8	209.0	20.6	27.5	101.0	93.4	1.4	2.6	13.4	38.5	-	1.4	4.0	17.4	55.9	-	KAQ
9	635.9	1268.0	400.6	20.8	54.0	0.8	1.9	1.3	7.7	-	0.8	2.7	4.0	11.7	-	AKH
10	497.4	44.0	71.5	146.3	73.2	2.6	2.1	11.7	36.8	-	2.6	4.8	16.5	53.3	-	HAQ
11	233.1	237.0	70.6	148.4	157.4	1.1	4.6	23.1	38.7	-	1.1	5.7	28.9	67.6	-	KAH
12	846.6	1397.7	182.1	209.6	308.5	1.0	2.6	39.4	53.0	-	1.0	3.6	43.0	96.0	-	KHH
13	469.1	2063.2	77.0	105.9	-	0.6	1.7	48.2	-	-	0.6	2.3	50.5	-	-	KH
14	1458.1	7802.1	278.6	85.7	128.4	0.5	1.2	2.5	42.7	-	0.5	1.7	4.2	46.9	-	KQH
15	1353.9	34.0	56.4	100.1	153.9	1.0	3.6	15.4	37.6	-	1.0	4.6	20.0	57.6	-	HAH

**Table 3:** Result of petro – physical properties of groundwater potential in North bank, Makurdi

VES	$\rho_a$ ( $\Omega m$ )	$h_a$ (m)	S ( $\Omega^{-1}$ )	T ( $\Omega m^2$ )	H (m/day)	$T_r$ ( $m^2/day$ )	$\phi$ (%)	Coefficient of permeability ( $K_p$ ) m/day	Protective capacity rating	Curve type
1	88.30	155.60	1.76	13739.48	5.91	920.02	33.50	2.76	Good	KAQ
2	145.70	36.30	0.25	5288.91	3.71	134.53	31.40	1.40	Moderate	QH Q
3	84.80	18.60	0.22	1577.28	6.14	114.21	33.67	2.95	Moderate	QH H
4	27.60	16.50	0.60	455.40	17.50	288.67	38.38	2.32	Moderate	KAH
5	59.60	97.00	1.63	5781.20	8.53	827.57	35.15	10.94	Good	QH Q
6	37.60	63.30	1.68	2380.08	13.11	829.96	37.08	12.47	Good	QH Q
7	67.60	39.00	0.58	2636.40	7.60	295.85	34.62	4.95	Moderate	KAH
8	101.00	38.50	0.38	3888.50	5.22	200.82	32.93	5.26	Moderate	KAQ
9	20.80	7.70	0.37	160.16	22.78	175.39	39.57	14.32	Moderate	AKH
10	146.30	36.80	0.25	5383.84	3.69	135.86	31.378	7.31	Moderate	HAQ
11	148.40	38.70	0.26	5743.08	3.64	140.98	31.32	30.25	Moderate	KAH
12	209.60	53.00	0.25	11108.80	2.64	139.91	29.87	20.00	Moderate	KHH
13	77.00	48.20	0.63	3711.40	6.72	323.82	34.07	26.21	Moderate	KH
14	85.70	42.70	0.50	3659.39	6.08	259.61	33.62	24.00	Moderate	KQH
15	100.10	37.60	0.38	3763.76	5.26	197.77	32.97	7.31	Moderate	HAH

**Table 4:** Results of physio-chemical characteristics of Groundwater in North Bank, Makurdi

Sample ID	Temperature (°C)	P <sup>H</sup>	TDS (mg/l)	EC (µS/cm)	Turbidity (NTU)	Total Hardness (mg/l)	Ca <sup>2+</sup> (mg/l)	Mg <sup>2+</sup> (mg/l)	Fe <sup>2+</sup> (mg/l)	Cu <sup>2+</sup> (mg/l)	Mn <sup>2+</sup> (mg/l)	Cl <sup>-</sup> (mg/l)	SO <sub>4</sub> <sup>2-</sup> (mg/l)	NO <sub>3</sub> <sup>-</sup> (mg/l)	NO <sub>2</sub> <sup>-</sup> (mg/l)
J1	26.70	7.25	260.00	400.00	2.34	130.00	50.00	60.00	0.01	0.04	0.15	160.00	60.00	24.00	0.45
J2	29.20	6.98	280.00	340.00	0.65	125.00	40.00	24.00	0.08	0.08	0.10	180.00	95.00	40.00	0.25
J3	29.50	6.71	300.00	400.00	0.35	127.00	45.00	35.00	0.01	0.03	0.20	160.00	80.00	35.00	0.30
J4	27.00	6.51	250.00	320.00	0.45	131.00	30.00	28.00	0.02	0.06	0.40	170.00	60.00	22.00	0.34
J5	26.00	7.82	150.00	250.00	14.5	165.00	50.00	30.00	0.04	0.15	0.45	151.00	60.00	24.00	0.15
J6	30.60	6.93	210.00	350.00	35.6	120.00	25.00	35.00	0.03	0.09	0.32	200.00	80.00	26.00	0.29
J7	31.50	6.77	240.00	450.00	26.4	120.00	40.00	36.00	0.04	0.08	0.24	300.00	80.00	25.00	0.50
J8	32.30	6.82	228.00	574.00	27.5	160.00	45.00	30.00	0.05	0.10	0.28	400.00	91.00	30.00	0.49
J9	32.70	6.73	66.30	132.00	0.45	30.00	14.00	8.00	0.04	0.11	0.13	110.00	31.00	12.00	0.02
J10	32.60	7.23	224.00	448.00	13.37	165.00	48.00	31.00	0.11	0.06	0.31	120.00	8.00	34.00	0.08

**Table 5:** Summary of statistics of physio-chemical parameters of groundwater samples (hand dug wells and boreholes) in North Bank, Makurdi

Parameter	Minimum	Maximum	Mean	Median	NAFDAC/WHO, 2015
Temperature (°C)	26.00	32.70	29.81	28.30	25
P <sup>H</sup>	6.51	7.25	6.98	7.38	6.50-8.50
TDS	66.30	300.00	220.83	180.00	500
EC (µS/cm)	132.50	574.00	366.40	300.00	1000
Turbidity (NTU)	0.35	35.60	12.16	25.10	5.0
Total Hardness	30.00	165.00	127.30	142.50	100
Ca <sup>2+</sup>	14.00	50.00	38.70	37.50	75
Mg <sup>2+</sup>	8.00	60.00	31.70	32.50	20
Fe <sup>2+</sup>	0.01	0.11	0.04	0.04	0.3
Cu <sup>2+</sup>	0.03	0.15	0.08	0.12	1.0
Mn <sup>2+</sup>	0.10	0.45	0.26	0.39	2.0
Cl <sup>-</sup>	110.00	400.00	195.12	175.00	100
SO <sub>4</sub> <sup>2-</sup>	8.00	95.00	64.50	70.00	100
NO <sub>3</sub> <sup>-</sup>	12.00	40.00	27.20	25.00	10
NO <sub>2</sub> <sup>-</sup>	0.02	0.50	0.29	0.22	0.02

**EC:** Electrical conductivity; **TDS:** Total Dissolved Solids; **NTU:** Nephelometric Turbidity Unit

The results of aquifer resistivity ( $\Omega m$ ) range from 20.80 to 209.60  $\Omega m$ , with an average value of 93.34  $\Omega m$ . Among the obtained results, VES 9 (Federal Housing Authority, North Bank) exhibits the lowest aquifer resistivity of 20.80  $\Omega m$ , while VES 12 (Okwute Well North Bank) records the highest aquifer resistivity value of 209.60  $\Omega m$ . The low aquifer resistivity in the study area is likely attributed to the presence of porous sandstone, indicating a saturated and more conductive layer<sup>34, 35, 36</sup>.

Figure 9a presents a 2D contour map illustrating the variation in aquifer resistivity across the study area. It reveals high resistivity in the southwestern part (VES 10, 11, and 12) and low resistivity in the southeastern part of the study area. The region with low resistivity may be attributed to the presence of highly conductive geomaterials, such as sandstone intercalated with clay and shale<sup>35</sup>. This condition could result in poor groundwater quality, as clay and shale tend to release magnesium and calcium ions into water, causing water hardness, consistent with laboratory results for water hardness.

Aquifer thickness ranges from 7.70 to 155.60 m, with an average value of 44.47 m (refer to Table 2). The notably high aquifer thickness of 155.60 m at VES 1 (UAM College of Science Block, South Core) suggests that this aquifer layer is capable of storing and transmitting a substantial amount of groundwater. This implies that the aquifer layer at VES 1 is likely more prolific and desirable than at other VES points, indicating

good groundwater potential. Conversely, VES 9, with the lowest aquifer thickness of 7.70 m, suggests less favorable groundwater potential. Figure 7b illustrates the distribution of aquifer thickness in the study area, indicating that the southeastern part, covering VES 1, has high aquifer thickness, which gradually decreases towards the northern and southwestern parts of the study area. It can be inferred from the study that places in the southeastern part with relatively high aquifer thickness are likely to have high groundwater potential.

The values of longitudinal conductance (S) range from 0.22 to 1.76  $\Omega^{-1}$ , with an average value of 0.65  $\Omega^{-1}$  (Table 2). Longitudinal conductance values, which determine the protective capacity of the study area according to the ratings by Henri<sup>29</sup> and Abiola et al.<sup>28</sup>, provide insight into the aquifer's protective capacity. The results categorize the study area as having both good and moderate protective capacity based on the numerical values assigned to each Vertical Electrical Sounding (VES) point. VES 1, 5, and 6 exhibit good aquifer protective capacity, likely due to the presence of clay and silt geomaterials, while other VES points show moderate protective capacity. It is observed that zones with high aquifer thickness are associated with good aquifer protective capacity, whereas zones with moderate protective capacity coincide with regions having lower thickness, making them more vulnerable to surface contamination due to the infiltration of contaminant fluid into the groundwater system. It can be inferred that high longitudinal conductance is influenced by relatively thick aquifer layers<sup>34,37,38,39</sup>. When compared with the classification proposed by Henri<sup>29</sup>, the study area has a moderate aquifer protective capacity, indicating that it is moderately vulnerable to contaminants based on the obtained results.

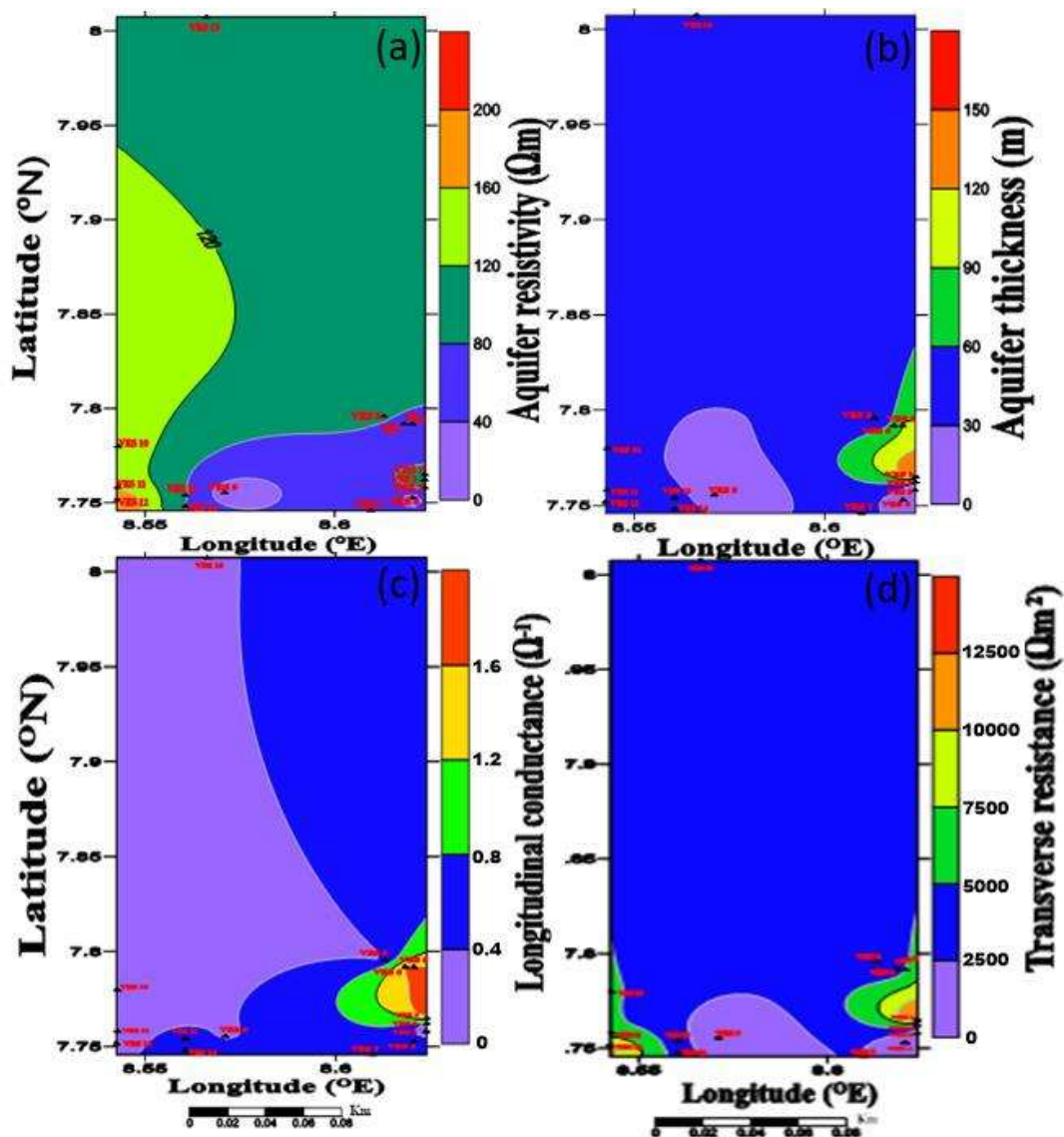


Figure 9: Contour map of aquifer resistivity, aquifer thickness, longitudinal conductance and transverse resistance in the study area

The estimated transverse resistance (T) values range from 160.16 to 13739.48  $\Omega\text{m}^2$ , with an average value of 4318.51  $\Omega\text{m}^2$ . Notably, the Federal Housing Authority, North Bank (VES 9), is observed to have the lowest transverse resistance value, while the UAM College of Science Block South Core (VES 1) boasts the highest transverse resistance value. The high transverse resistance aligns with a high aquifer layer thickness, indicating a region of high yield from the aquifer units. Conversely, low transverse resistance coincides with low aquifer layer thickness, signaling a lower aquifer yield<sup>37</sup>. Based on the results obtained in the study area, the generally high values of transverse resistance in most VES points suggest that the area has good groundwater potential, with exceptions noted for VES 4 and VES 9, which exhibit low values of transverse resistance, indicating low aquifer yield and transmissivity.

Figure 10a presents the spatial map of hydraulic conductivity (H), transmissivity, porosity, and coefficient of permeability. Hydraulic conductivity, providing insights into the water-producing capacities of the aquifer layer, was estimated using aquifer resistivity values. The results showcase high variability in H across the study area, ranging from 2.64 to 22.78 m/day, with an average value of 7.90 m/day. Notably, the lowest hydraulic conductivity of 2.64 m/day at VES 12 coincides with the highest aquifer resistivity, while the highest hydraulic conductivity of 22.78 m/day at VES 9 is associated with the lowest aquifer thickness. This indicates that low resistivity does not necessarily equate to low hydraulic conductivity, suggesting that hydraulic conductivity depends on factors such as the degree of saturation, intrinsic permeability of the geomaterials, and particle size distribution of geomaterials<sup>40</sup>. The results delineate that regions (VES 9, 6, 4, 5) with high hydraulic conductivity indicate the presence of prolific aquifers, although VES 9, with a very low aquifer thickness of 7.70 m, may not be able to store enough groundwater for economic use.

Aquifer transmissivity (Tr), which plays a crucial role in groundwater abstraction, has values ranging from 114.21 to 920.02  $\text{m}^2/\text{day}$  (refer to Table 2). Notably, VES 3 has the lowest transmissivity value (114.21  $\text{m}^2/\text{day}$ ), while VES 1 (UAM College of Science Block South Core, North Bank) boasts the highest transmissivity value (920.02  $\text{m}^2/\text{day}$ ), indicating that this location has a high water-bearing potential and is highly permeable to fluid movement. The contour map (Figure 10b) illustrates the variation of aquifer transmissivity across the study area, showcasing high transmissivity in the southeastern part. This zone with high transmissivity corresponds to a zone with high aquifer thickness, indicating that a zone with high aquifer thickness is likely to have high aquifer transmissivity, hence a prolific aquifer. The uneven distribution of changes in the water-bearing zones and their distribution depict the variational trend in size and potential of groundwater in the study area<sup>36</sup>.

Porosity plays a fundamental role as a transmitting property in groundwater availability, determining whether an aquifer is active or not. The estimated porosity ranges from 29.87% to 39.57%, with an average porosity value of 33.97%. The results indicate that Okwute Well North Bank (VES 12) has the lowest porosity value of 29.87%, while Our Lady of Fatima Primary School, North Bank (VES 9) has the highest porosity value of 39.57%. The aquifer layer may be classified as sand, sandstone, and gravel based on the range of porosity values obtained<sup>41,42</sup>. The contour map (Figure 10c) illustrates high aquifer porosity across the southeastern part of the study area, possibly due to high communicating pores and high storativity. It shows that as porosity increases, aquifer resistivity decreases, which may be attributed to the ratio of clay to sand mixture, suggesting the presence of argillites in the aquifer layer<sup>43</sup>.

The coefficient of permeability has values ranging from 1.40 to 30.25 m/day, with an average value of 11.50 m/day. The contour map (Figure 10d) reveals that permeability is high in the southwestern part of the study area and decreases towards other parts. It is observed that the zone with high permeability is also the zone with low longitudinal conductance. The uneven variation of permeability could be attributed to the grain sizes, pore shapes, size, and shape of the interconnections of the aquifer layer.

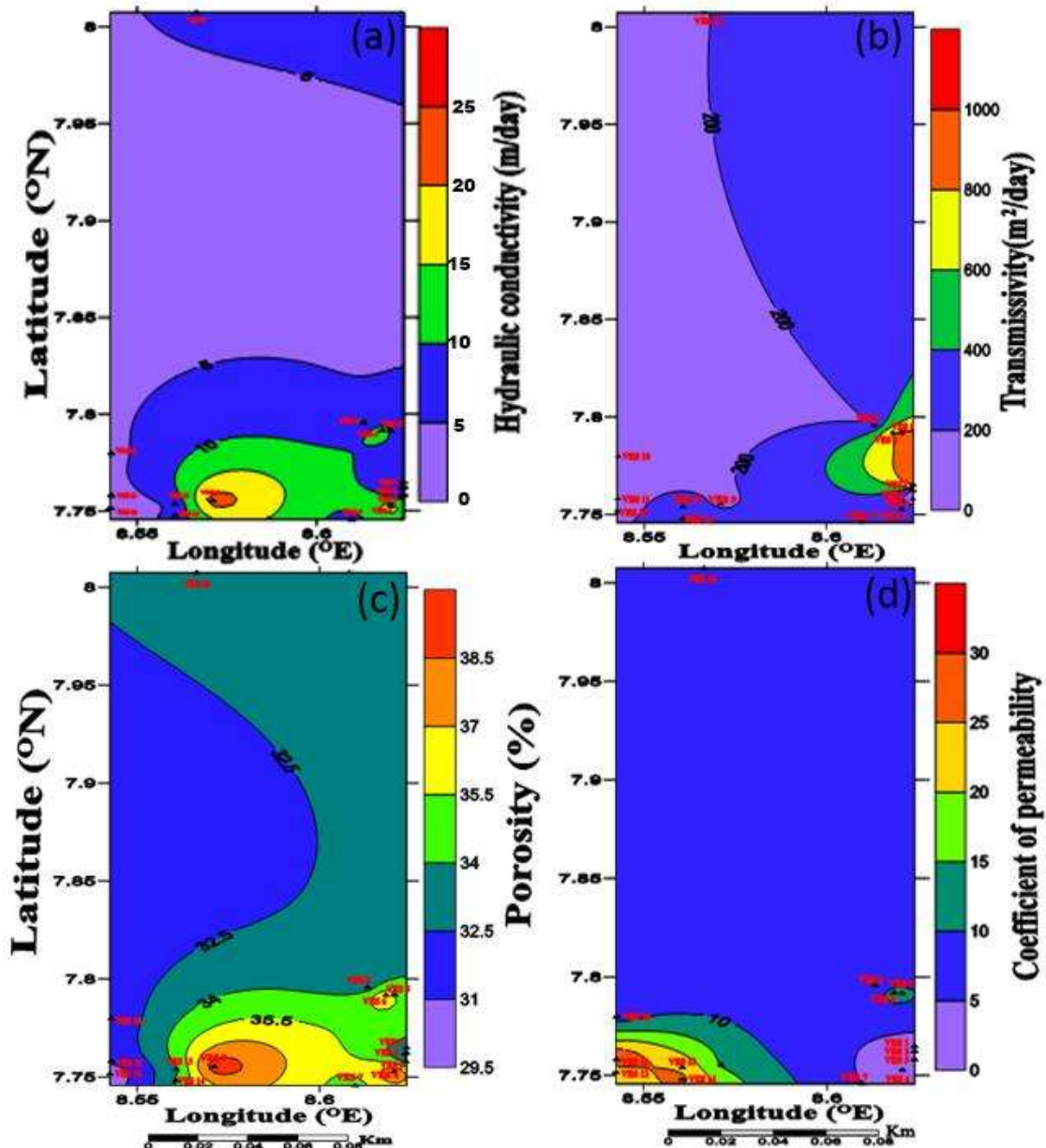


Figure 10 Spatial map of the hydraulic conductivity (H), transmissivity, porosity and coefficient of permeability.

The turbidity value ranges from 0.35 to 35.60 NTU, with a mean value of 12.6 NTU, contrasting with the recommended limit of 5.0 NTU by the National Agency for Food, Drug Administration and Control/World Health Organization<sup>32</sup>. Water samples from wells J5, J6, J7, J8, and J10 exceed the NAFDAC/WHO<sup>32,33</sup> standards; while others fall below the standard (Table 3 and Table 4). The observed high turbidity values may be attributed to unwanted materials entering these wells, especially during the dry season. Since these wells are not properly covered, runoff also enhances turbidity values.

Total dissolved solids (TDS) indicate the amount of dissolved substances in water, with a concentration ranging from 66.30 to 300 mg/l and a mean concentration of 220.83 mg/l. The electrical conductivity (EC) concentration varies from 132.50  $\mu\text{S}/\text{cm}$  to 574.00  $\mu\text{S}/\text{cm}$ , with an average value of 366.40  $\mu\text{S}/\text{cm}$  (refer to Table 3). The TDS and EC values are below the NAFDAC/WHO recommended limits of 500 mg/l for TDS and 1000  $\mu\text{S}/\text{cm}$  for conductivity<sup>32</sup>. EC and TDS serve as pollution tracers and important water quality indicators; hence, all the water samples in the study area fall below the recommended limits of NAFDAC/WHO<sup>32,33</sup>. This may be due to the infiltration of contaminants from dumpsites, soakaways, and herbicides into the subsurface<sup>44</sup>.

Temperature measures the degree of hotness or coldness of a material, while pH measures the hydrogen ion concentration of water. The pH values range from 6.51 to 7.25, while water temperature ranges from 26.00

°C to 32.70 °C. The pH falls within the acceptable range of 6.50 – 8.50, as recommended by NAFDAC/WHO<sup>32,33</sup>, while the temperature exceeded the NAFDAC/WHO recommended limit. These are crucial water quality indicators that play important roles in the dissolution of substances in water. Chemical substances dissolve more readily in water under low pH and high-temperature conditions.

The water samples were also analyzed to determine the concentration of chemical parameters. Total hardness ranges between 30.00 mg/l and 165.00 mg/l, with an average value of 127.30 mg/l. It is observed that all the wells have concentrations above the recommended limits of NAFDAC/WHO<sup>32,33</sup>, except well J9. The presence of calcium and magnesium ions in water is believed to be responsible for water hardness. Hardness wastes a lot of soap and forms scum in kettles that need to be removed before use. All the water samples analyzed are hard except dug well J9 (LGEA Primary School, North Bank).

The concentration of copper, calcium, manganese, and iron in the water samples ranges from 0.03 to 0.15 mg/l; 14.00 to 50 mg/l; 0.10 to 0.45 mg/l; and 0.01 to 0.11 mg/l, respectively. The concentration of these ions falls below the NAFDAC/WHO recommended limit for drinking water; this could be due to the low/absence of minerals bearing these ions in the subsurface<sup>42</sup>. The concentration of magnesium in water samples ranges from 8.00 to 60 mg/l; it exceeded the NAFDAC/WHO standard in the wells except well J9. This result corresponds to that of total hardness where all the wells except J9 exceeded the NAFDAC/WHO acceptable limit, hence the hardness of water in those region<sup>33</sup>. The concentration of sulfate ion is below the recommended limit of NAFDAC/WHO in all the water samples analyzed. The sulfate concentration ranges from 8.00 to 95 mg/l, which is below the NAFDAC/WHO limit of 100 mg/l. Nitrate (NO<sub>3</sub><sup>-</sup>), nitrite (NO<sub>2</sub><sup>-</sup>), and chloride (Cl<sup>-</sup>) ions have values above the permissible limits of NAFDAC/WHO<sup>32,33</sup>. Nitrate values range from 12 to 40 mg/l against 10 mg/l, nitrite values range from 0.02 to 0.05 mg/l as against the recommended limit of 0.02 mg/l, while chloride concentration ranges from 110 to 400 mg/l against the permissible limit of 100 mg/l<sup>32</sup>. High concentrations of chloride in water may be attributed to the poor sanitary conditions of the wells and may cause blue baby syndrome in children.

## VII. Conclusion

This study has produced a more detailed knowledge of the subsurface environment and groundwater potential in the studied area. The shift in soil texture from sandy loam to sandy clay loam with depth emphasizes the significance of taking vertical variability into account when defining the soil profile. Vertical Electrical Soundings (VES) geo-electric studies revealed a complex underlying structure with many strata, each with individual resistivities. The existence of an aquifer layer with variable resistivity values indicates the presence of porous sandstone, which has a substantial impact on groundwater conductivity.

The computation of hydrogeological parameters, including longitudinal conductance, transverse resistance, hydraulic conductivity, transmissivity, porosity, and coefficient of permeability, offers quantitative insights into the protective capacity and yield potential of the aquifer. The observed correlation between aquifer thickness and protective capacity emphasizes the relevance of subsurface characteristics in determining groundwater vulnerability to contaminants. The spatial distribution maps provide a visual representation of the variations in hydraulic conductivity, transmissivity, and porosity, aiding in the identification of zones with high groundwater potential.

The groundwater quality assessment highlights both compliance and non-compliance with recommended standards. Turbidity values exceeding limits in some wells suggest potential contamination, particularly during the dry season. However, overall compliance with total dissolved solids, electrical conductivity, and pH standards indicates a baseline level of water quality in the study area.

The integration of electrical resistivity tests and permeability pits enhances the reliability and robustness of our findings, offering a multi-faceted approach to subsurface characterization. These findings contribute valuable information for sustainable water resource management, aiding in decision-making processes for environmental planning and groundwater utilization. The identification of zones with high groundwater potential provides a basis for targeted resource allocation and infrastructure development, ensuring the responsible and effective use of this vital natural resource.

## References

- [1]. Arulbalaji P, Padmalal D, Sreelash K. GIS And AHP Techniques Based Delineation Of Groundwater Potential Zones: A Case Study From Southern Western Ghats, India. *Scientific Reports*. 2019; 9.
- [2]. Gleeson T, Cuthbert MO, Ferguson GA, Perrone D. Global Groundwater Sustainability, Resources, And Systems In The Anthropocene. *Annual Review Of Earth And Planetary Sciences*. 2019
- [3]. Edet A, Okereke CS. Hydrogeologic Framework Of The Shallow Aquifers In The Ikom – Mamfe Embayment, Nigeria Using An Integrated Approach. *Journal Of African Earth Sciences*. 2014; 92:25 – 44.
- [4]. Perdomo S, Ainchoil JE, And Kruse E. Hydraulic Parameters Estimation From Well Logging Resistivity And Geoelectrical Measurements. *Journal Of Applied Geophysics*, 2014; 105:50 – 58
- [5]. Anomoharan O. Assessment Of Groundwater Potential And Aquifer Characteristics In The Vicinity Of Igun, Eku And Oria In Delta State, Nigeria. *Journal Of Water Resources And Protection* 2014; (6):731 – 740.

- [6] Lowrie W. Fundamentals Of Geophysics. United Kingdom: Cambridge University Press. 2004
- [7] Ibrahim E. Geoelectric Resistivity Survey For Site Investigation In East Matruh Area, North Western Desert, Egypt. World Applied Sciences Journal, 2013; 21 (7):1008 – 1016.
- [8] Aanuoluwa AT, And Ayobami SL. Geoelectric Assessment Of Groundwater Prospect And Vulnerability Of Overburden Aquifers At Adamasun Area, Oniye, Southwestern Nigeria. Archives Of Applied Science Research. 2012; 4(5): 2077–2093.
- [9] Anomohanran O. Hydrogeophysical And Hydrogeological Investigations Of Groundwater Resources In Delta Central, Nigeria. Journal Of Taibah University For Science, 2015; 9(1): 57 – 68
- [10] Hrudey SE, Hrudey EJ. Safe drinking water: lessons from recent outbreaks in affluent nations. London, UK: IWA Publishing. 2004
- [11] Allen MJ, Edberg SC, Clancy J, Hrudey SE. Drinking water microbial myths - a primer for utility managers, engineers and non-microbiologists. 15th National Conference & 6th Policy Forum on Drinking Water Kelowna, B. C. 2012.
- [12] Onyango AE, Okoth MW, Kunyanga CN, Aliwa BO. Microbiological Quality and Contamination Level of Water Sources in Isiolo County in Kenya. J Environ Public Health. 2018; 2139867. doi: 10.1155/2018/2139867.
- [13] Edet AE. Vulnerability evaluation of coastal plain sand aquifer with a case example from Calabar, South- Eastern Nigeria. J. Environ. Geol. 2004; 45: 1062–1070.
- [14] Amadi AN, Nwawulu CD, Unuevho CI, Okoye NO, Okunlola IA, Egharevba NA, Ako TA, Alkali YB. Evaluation of Groundwater potential in Pompo village, Gidan Kwano, Minna using vertical electrical resistivity sounding. British Journal of Applied Science and Technology. 2011; 1(3): 53 – 66.
- [15] Adeniji AE, Obiora ON, Omonona OV, Ayuba R. Geoelectrical evaluation of groundwater potentials of Bwari basement area, North central Nigeria. 2013; 8(25): 1350 – 1361.
- [16] Akande WG, Idris – Nda A, Amadi AN, Abdulftai IA, Alabi AA, Yahaya I. Evaluation of Groundwater potential of Chanchaga area, Minna, North central Nigeria. American Journal of innovative research and applied sciences. 2016; 2(1): 1 - 9.
- [17] Onimisi M, Kolawole M, Daniel A, Ebeh A. Vertical Electrical Sounding survey for groundwater exploration in parts of Anyiba and its environs in the Anambra Basins of Nigeria. British Journal of Applied Science and Technology. 2014; 4(13): 1978 – 1988
- [18] Obiora, DN, Ajala AE, Ibuot JC. Evaluation of Aquifer protective of overburden unit and soil corrosivity in Makurdi, Benue state, Nigeria, using Electrical Resistivity Method. Journal of Earth System Science, 2015; 124(1):125 – 135.
- [19] Obriake, SE, Oleka AB, Ojuola BS, Anudu GK, Kana MA, Iliya MM. Hydro-Geophysical Assessment of Groundwater Potential and Aquifer Vulnerability of the Turonian Makurdi Formation in North Bank area, Makurdi, Middle Benue Trough, Journal of Mining and Geology. 2022; 58(1): 189 – 201
- [20] Ayaakaa DT, Ikogo, SO, Adagba G, Shiada, SM, Bem TT. (2023). Geoelectrical Assessment Of Groundwater Potentials Of Some Parts Of Makurdi Metropolis, Benue State Using The Dar Zarrouk Parameters. IOSR Journal of Applied Physics (IOSR-JAP), 2023;15(3): 52-61. DOI: 10.9790/4861-1503015261
- [21] Akuh TI. Hydrogeology and Groundwater Quality in Makurdi Metropolis and its Environs, Part of Makurdi (Sheet 251), North Central Nigeria. Unpublished Masters' Thesis, Ahmadu Bello University, Zaria. 2011.
- [22] Musa ST. Geology and Hydrogeology of Part of Makurdi Sheet 251 SW, North Central Nigeria, Unpublished Masters' thesis, Federal University of Technology, Minna. 2017
- [23] Offodile ME. The occurrence and exploitation of groundwater in Nigeria basement complex. J. Minner Geol. 1983; 20: 131 – 146.
- [24] Hengl T (2018). Soil texture classes (USDA system) for 6 soil depths (0, 10, 30, 60, 100 and 200 cm) at 250 m (Version v02) [Data set]. Zenodo.
- [25] Ezema P. Fundamentals of Applied Geophysics. Rejoint Communication services Ltd. Enugu, Nigeria. 2005
- [26] Telford WM, Geldart IP, Sheriff RE. Applied Geophysics, 2nd ed., Cambridge University Press. New York. 1990
- [27] Heigold PO, Gilkeson RH, Cartwright K, Reed PC. Aquifer transmissivity from surficial electrical methods. Groundwater, 1979;17(4):338 – 345.
- [28] Abiola O, Enikanselu PA, Oladapo MI. Groundwater potential and aquifer protective capacity of overburden units in Ado-Ekiti, Southwestern Nigeria. International Journal of Physical Sciences. 2009; 4(3): 120 – 132
- [29] Henriot, JP. Direct application of Dar Zarouk parameters in groundwater survey. Geophysics Prospecting, 1976; 24:344 – 353
- [30]. Todd DK 1980. Groundwater Hydrology, 2nd edition. xiii 535 pp., numerous figs and tables. New York, Chichester, Brisbane, Toronto: John Wiley. 1980 . ISBN 0 471 87616 X
- [31]. Trishna B. Permeability of soils: Factors and Determination. Soil Management. 2019
- [32]. National Agency for Food and Drug Administration and Control (NAFDAC). Guideline for Drinking Water Quality, 2015; 1
- [33]. World Health Organization (WHO) Guideline for Drinking Water Quality. 2015;1
- [34]. Obiora, DN, Adeolu EA, Ibuot JC. Investigation of groundwater flow potential in Makurdi, North central Nigeria, using surficial electrical resistivity method. African Journal of Environmental Sciences and Technology. 2015; 9(9): 723 – 733.
- [35]. Alile OM, Ujuanbi O, Evbuomwam IA. Geoelectric investigation of Groundwater in Obaretin Iyanomon Locality, Edo State, Nigeria, Journal of Geology and Mining Research. 2011;3(1), 13-20.
- [36]. Aleke CG, Ibuot JC, Obiora DN Application of electrical resistivity method in Estimating geohydraulic properties of a sandy hydroclithofacies: a case study of Ajali Sandstone in Ninth Mile, Enugu State, Nigeria. Arab J Geosci. 2018;11:322.
- [37]. George JN, Ibuot JC, Obiora DN. Geoelectrohydraulic of shallow sandy in Itu, Akwa Ibom State (Nigeria) using geoelectric and hydrogeological measurements. Journal of African Earth Sciences, 2015;110: 52-63
- [38]. Ibang J, George NJ. Estimating geohydraulic parameters, protective strength and corrosivity of hydrogeological Units: a case study of ALSCON Ikot Abasi Southern Nigerian. Arabian Journal of Geoscience. 2016; 9(5): 1-16
- [39]. Ibuot, JC, Obiora DN. Geophysical assessment of aquifer vulnerability and management: a case study of University of Nigeria, Nsukka, Enugu state. Journal of Applied water science. 2020;10-29.
- [40]. Niwas S, Celik M. Equation estimation of porosity and hydraulic conductivity of Ruhrtal aquifer in Germany using near surface geophysics. Journal of Applied Geophysics, 2012; 84, 77–85. doi:10.1016/j.jappgeo.2012.06.001
- [41]. Driscoll FD Groundwater and wells. St. Paul, MN: Johnson Screens. 1986
- [42]. Freeze RA, Cherry JA Groundwater. NJ: Prentice Hall. 1979
- [43] Ibuot JC, George NJ, Okwesili AN, Obiora DN. Investigation of litho-textural characteristics of aquifer in Nkanu West Local Government Area of Enugu state, southeastern Nigeria. J Afr Earth Sci. 2019; 157:197–2017
- [44]. Barker R, Rao TV, Thangarajan M. Delineation of contaminant zone through electrical imaging technique. Current Science, 2001; 81(3): 277-283.